

## Experimental invalidation of phase-transition-induced elastic softening in CrN

Shanmin Wang,<sup>1,2</sup> Xiaohui Yu,<sup>2</sup> Jianzhong Zhang,<sup>2</sup> Miao Chen,<sup>1</sup> Jinlong Zhu,<sup>2</sup> Liping Wang,<sup>3</sup> Duanwei He,<sup>1,\*</sup> Zhijun Lin,<sup>2</sup> Ruifeng Zhang,<sup>4</sup> Kurt Leinenweber,<sup>5</sup> and Yusheng Zhao<sup>2,3,\*</sup>

<sup>1</sup>*Institute of Atomic & Molecular Physics, Sichuan University, Chengdu 610065, People's Republic of China*

<sup>2</sup>*LANSCE Division, Los Alamos National Laboratory, Los Alamos, New Mexico 87545, USA*

<sup>3</sup>*HiPSEC, University of Nevada, Las Vegas, Nevada 89154, USA*

<sup>4</sup>*Theoretical Division, Los Alamos National Laboratory, Los Alamos, New Mexico 87545, USA*

<sup>5</sup>*Department of Chemistry and Biochemistry, Arizona State University, Tempe, Arizona 85287, USA*

(Received 10 May 2012; revised manuscript received 6 August 2012; published 28 August 2012)

We report experimental results of phase stability and incompressibility of CrN. The obtained bulk moduli for cubic and orthorhombic CrN are 257 and 262 GPa, respectively. These results invalidate the conclusion of phase-transition-induced elastic softening recently reported based on nonmagnetic simulations for cubic CrN [*Nature Mater.* **8**, 947 (2009)]. On the other hand, they provide the only experimental evidence to support the computational models involving the local magnetic moment of Cr atoms [*Nature Mater.* **9**, 283 (2010)], indicating that atomic spin has a profound influence on the material's elastic properties. We also demonstrate that nonstoichiometry in CrN<sub>x</sub> has strong effects on its structural stability.

DOI: 10.1103/PhysRevB.86.064111

PACS number(s): 62.20.-x, 75.10.-b, 75.20.Hr

### I. INTRODUCTION

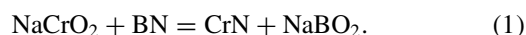
Among transition-metal nitrides, chromium nitride (CrN) exhibits fascinating structural, magnetic, and electronic properties that are of fundamental importance to condensed-matter and computational physics.<sup>1-5</sup> At atmospheric pressure, CrN possesses an orthorhombic (*orthor*) structure and a unique antiferromagnetic ordering below the Néel temperature ( $T_N$ ) of 286 K; it transforms into a cubic (*c*), paramagnetic configuration above  $T_N$ .<sup>1</sup> Recent studies on CrN provide new insight into structural transition that is driven by magnetic ordering.<sup>2</sup> The magnetic moment also plays crucial roles in a variety of physical phenomena in other material systems. For example, Mott transition in MnO (Ref. 6) and elastic hardening in (Fe<sub>x</sub>Mg<sub>1-x</sub>)O (Ref. 7) are commonly attributed to the collapse of the magnetic moment under high-pressure conditions. However, first-principles calculations for paramagnetic materials are typically performed without considering local magnetic moments associated with atomic spin. As a result, the calculations for paramagnetic materials are often inconsistent with experimental observations. The experimentally reported bulk moduli for paramagnetic *c*-CoO and *c*-PbCrO<sub>3</sub>, for example, are 180 and 59 GPa, respectively, which are 70% and 290% lower than calculated values of 307 and 230 GPa using nonmagnetic simulation.<sup>8,9</sup> Conflicting electronic properties have also been predicted for cubic paramagnetic CrN by first-principles calculations, including a metal, a semiconductor, or an insulator.<sup>2,4,5</sup>

The impacts of magnetostructural phase transition on elastic properties and electrical conductivity have recently been the subjects of intense research for a wide range of materials, including CrN,<sup>2,10,11</sup> TiN,<sup>12</sup> MnO,<sup>6</sup> Fe<sub>2</sub>O<sub>3</sub>,<sup>13</sup> Fe<sub>x</sub>Mg<sub>1-x</sub>O,<sup>7</sup> Fe<sub>x</sub>Mg<sub>1-x</sub>SiO<sub>3</sub>,<sup>14,15</sup> and PbCrO<sub>3</sub>.<sup>9</sup> In particular, Rivadulla *et al.* reported unprecedented elastic softening in CrN with the bulk modulus  $B_0$  of the high-pressure orthorhombic phase that is 25% smaller than that of the low-pressure cubic phase.<sup>10</sup> Because these authors were unable to experimentally determine  $B_0$  for the *c*-CrN due to its limited structural stability (i.e., stable only up to 1 GPa), their conclusion was

mainly based on first-principles calculations that predicted a high  $B_0$  of 340 GPa using a nonmagnetic model.<sup>10</sup> The computational scheme applied in Ref. 10, however, was critically questioned by Alling *et al.* (2010) who obtained a substantially lower value of  $B_0 = 252$  GPa when the local magnetic moment was introduced into the simulation package for the paramagnetic/cubic phase.<sup>11</sup> To date, the controversy between theories has yet to be resolved,<sup>16</sup> calling for more a rigorous experimental elucidation of this intriguing phenomenon. Here, we report experimental results of incompressibility and phase stability of CrN based on high-pressure ( $P$ ) synchrotron x-ray and time-of-flight neutron-diffraction and electrical resistivity measurements at low temperatures ( $T$ ).

### II. EXPERIMENTAL DETAILS

Stoichiometric CrN was prepared by a solid-state ion-exchange reaction between NaCrO<sub>2</sub> and *h*BN at 5 GPa and 1573 K for 20 min, which is given by



The unwanted by-product NaBO<sub>2</sub> can be readily removed by washing the reaction product in water, leading to nearly phase-pure *c*-CrN. The experimental details can be found in Ref. 17. Using similar reaction routes, we also successfully prepared nitrogen-rich tungsten nitrides (W<sub>2</sub>N<sub>3</sub>) and molybdenum nitrides (MoN<sub>2</sub>),<sup>18</sup> indicating that our formulated solid-state ion-exchange reaction is an effective route to synthesize nitrogen-rich nitrides.

The experimentally run products were characterized by x-ray diffraction (XRD) and time-of-flight neutron diffraction. Rietveld refinements were performed by using GSAS software.<sup>19</sup> X-ray photoelectron spectroscopy was used to determine stoichiometric composition. The Cr:N molar ratio was very close to 1:1 for the sample prepared by reaction (1). The sample density was determined using the Archimedes method on the bulk CrN samples sintered at 8 GPa and 2073–2273 K for 45 min. The measured densities are typically

within 95% of the x-ray density. The sintered samples were characterized by x-ray diffraction; all final products for *c*-CrN were well crystallized and nearly phase pure. These combined characterizations indicate that our high-*P* synthetic route presents significant advantages over traditional synthetic methods.<sup>10,20</sup>

Low-temperature electrical resistivity measurements were performed at ambient pressure on well-sintered CrN. The mirror-quality surfaces were prepared for the four-point electrical measurement. Compression experiments on CrN were conducted at pressures up to 40 GPa and temperatures in the range of 300–1200 K, using angular- and energy-dispersive synchrotron x-ray diffraction and time-of-flight neutron scattering. We used a diamond-anvil cell (DAC) for angular-dispersive experiments performed at the HPCAT 16BM-D beamline of Argonne National Laboratory. Neon served as the pressure-transmitting medium. Several ruby crystals were mounted inside the gasket hole to serve as internal pressure standards. Experimental details can be found elsewhere.<sup>9</sup> For energy-dispersive experiments, we used a DIA-type large-volume high-pressure apparatus installed at the X17B2 beamline of the National Synchrotron Light Source, Brookhaven National Laboratory. The experimental details of this paper are similar to those described in Ref. 21. We first compressed the pressure cell to 8.7 GPa at room temperature, followed by heating to the maximum temperature of 1200 K, and subsequent cooling to 1000, 800, 600, 400, and 300 K, respectively. XRD diffraction data were collected on cooling to minimize nonhydrostatic stress built up during the room-temperature compression. The same procedures were repeated at progressively lower pressures. High-*P-T* neutron-scattering experiments were performed in a TAP-98 toroidal-anvil press at Lujan Neutron Scattering Center, Los Alamos Neutron Science Center.<sup>22</sup> In the latter two types of experiments, NaCl was used as an internal pressure standard with pressures calculated using a Decker scale.<sup>23</sup>

### III. RESULTS AND DISCUSSION

Figure 1 shows XRD patterns collected at ambient conditions and at 11.3 GPa. The refined ambient lattice parameter for *c*-CrN is  $a = 4.1513(2)$  Å, which is 0.08% larger than reported by Rivadulla *et al.* (4.1480 Å) for the sample synthesized by ammonolysis of Cr<sub>3</sub>S<sub>4</sub>.<sup>10</sup> To understand this small but conceivably meaningful difference, we subjected the high-*P* synthesized CrN to a high-*T* treatment at 1473 K for 1 h in an Ar atmosphere. To our delight, we recovered a CrN sample with  $a = 4.1481$  Å; quite obviously, the observed reduction in the lattice parameter can be attributed to nitrogen degassing at elevated temperatures. Based on this finding, we infer that the sample synthesized by Rivadulla *et al.* (2009) is nitrogen deficient with  $x < 1$  in CrN<sub>*x*</sub>.<sup>10</sup> At 11.3 GPa, the lattice parameters are  $a = 5.684$ ,  $b = 2.937$ , and  $c = 4.082$  Å, corresponding to an x-ray density of 6.433 g/cm<sup>3</sup> [Fig. 1(b)]. The refined atomic positions are given below,

$$\begin{aligned} \text{Cr} : (x, 1/4, z), \text{ Wyckoff site } 4c, \quad x = 0.1135, \text{ and } z = 1/4; \\ \text{N} : (x, 1/4, z), \text{ Wyckoff site } 4c, \quad x = 0.1155, \text{ and } z = 3/4. \end{aligned}$$

Our refined *x* positions for Cr and N are different from those of Corliss *et al.*<sup>1</sup> who proposed  $x = 1/8$  for both Cr

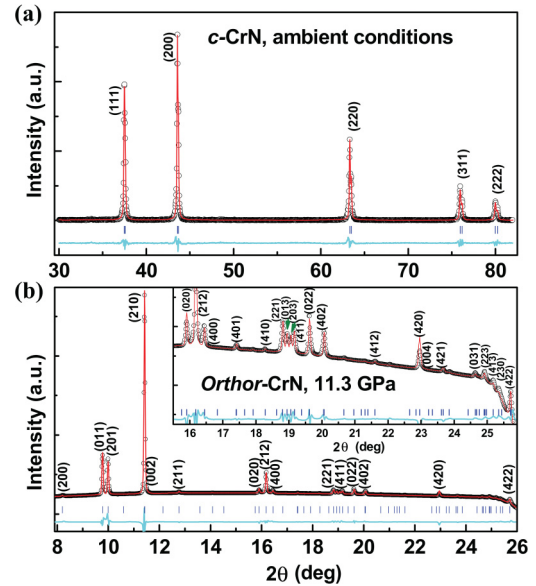


FIG. 1. (Color online) Refined XRD patterns for CrN. (a) The ambient pressure pattern of *c*-CrN was collected with a copper target ( $\lambda K\alpha_1 = 1.54056$  and  $\lambda K\alpha_2 = 1.54440$  Å). (b) The synchrotron XRD pattern for *orthor*-CrN was collected at 11.3 GPa with a wavelength of 0.40662 Å. Black circles and red lines denote the observed and calculated profiles, respectively. The difference curve between the observed and the calculated profiles is shown in cyan (bottom of each panel). The blue tick marks correspond to the peak positions.

and N. However, because (200) and (211) peaks are observed in our XRD pattern, Cr and N should have different *x* values.

Figure 2(a) shows typical angular-dispersive XRD patterns collected at room temperature in a DAC experiment. The onset pressure for the cubic-orthorhombic phase transition was determined to be  $\sim 4.9$  GPa with the two CrN phases coexisting up to  $\sim 7.5$  GPa. Consistent with these findings, we observed the cubic-to-orthorhombic phase transition at 5.3 (4) GPa in high-*P-T* energy-dispersive synchrotron experiments using a large-volume apparatus. We also conducted high-pressure neutron-diffraction experiments on CrN; at pressures up to 2.0 GPa, neither structural phase transition nor magnetic transition to an antiferromagnetic phase was observed at room temperature. These observations are markedly different from the commonly accepted value of 1 GPa for the cubic-to-orthorhombic phase transition in CrN.<sup>10,11</sup> To further map out the phase boundary for CrN, we carefully monitored the orthorhombic-cubic transition above room temperature. Shown in Figs. 2(b) and 2(c) are XRD patterns collected at selected high-*P-T* conditions. Based on these observations, the transition pressures are determined to be 5.46 GPa at 315 K and 8.87 GPa at 358 K.

The low-*T* electrical resistivity measurements on well-sintered CrN show an abrupt drop near 240 K at atmospheric pressure [inset in Fig. 2(d)], which corresponds to the cubic-to-orthorhombic phase transition. Both of these two phases are intrinsic metals, indicating that previously reported conflicts in electronic properties may be associated with crystalline disorders. The detailed discussion of these observations will be published elsewhere. This temperature is substantially

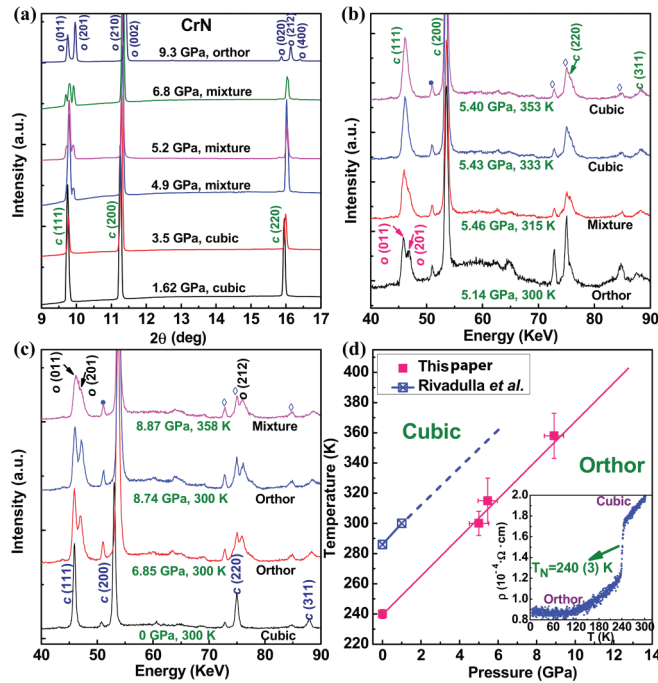


FIG. 2. (Color online) Phase stability determined based on compression experiments and low- $T$  electrical resistivity measurements. (a) Selected high- $P$  angular-dispersive synchrotron XRD patterns collected in the DAC at room temperature. The wavelength is  $0.40662 \text{ \AA}$ . (b) and (c) Energy-dispersive synchrotron x-ray diffraction patterns at selected  $P$ - $T$  conditions. At  $315 \text{ K}$ , *orthor*-to-*cubic* transition happens at  $5.46 \text{ GPa}$ ; the transition pressure increases to  $8.87 \text{ GPa}$  at  $\sim 358 \text{ K}$ . Fluorescence peaks of Pb and Cr are denoted as blue diamonds and blue dots, respectively. (d) The orthorhombic-cubic phase-transition boundary determined by high- $P$ - $T$  synchrotron XRD and low- $T$  electrical resistivity measurements. The inset shows the electrical resistivity as a function of temperature. Phase transition happens at  $240 (3) \text{ K}$ .

lower than previously reported values of  $\sim 270$ – $286 \text{ K}$  for CrN samples prepared by traditional synthetic routes.<sup>1,24,25</sup> As pointed out by Filippetti *et al.*, nitrogen has a strong tendency to form dimers, which leads to difficulties in growing defect-free transition-metal nitrides using those approaches.<sup>3</sup> Earlier, we also showed that the CrN samples used in a previous paper (e.g., Ref. 10) are indeed nitrogen deficient with  $x < 1$  in  $\text{CrN}_x$ . These observations indicate that the Neel temperature in  $\text{CrN}_x$  may be sensitive to the degree of nonstoichiometry. On the other hand, as illustrated in Fig. 2(d), the determined transition temperature of  $240 (3) \text{ K}$  at ambient pressure lines up very well with the transition points observed under high- $P$ - $T$  conditions, allowing the phase boundary to be tightly constrained for stoichiometric CrN. Also plotted in Fig. 2(d) is the phase boundary derived from the results of Rivadulla *et al.* for nonstoichiometric  $\text{CrN}_x$  ( $x < 1$ ),<sup>10</sup> indicating that the presence of crystal defects promotes the transition to substantially lower pressures. Further experimental and computational work is warranted to quantify and to understand this effect. A particular area of focus in the experimental studies is the stoichiometric composition of  $\text{CrN}_x$ , which needs to be accurately determined and reported in future papers.

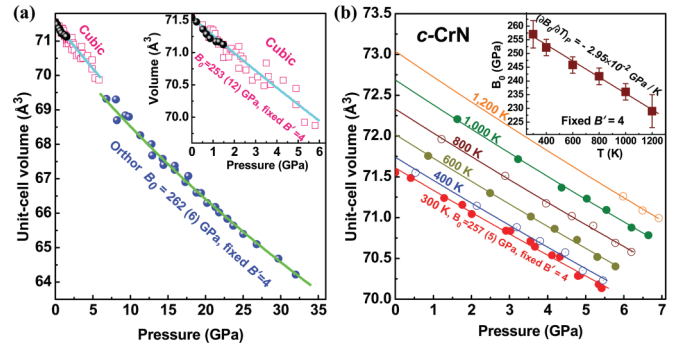


FIG. 3. (Color online) Results of compression experiments. (a) Volume-pressure data of *cubic*- (open pink squares) and *orthorhombic*-CrN (solid blue circles) collected at room temperature using angular-dispersive high- $P$  synchrotron XRD in a DAC. The inset is an enlarged portion of data for *c*-CrN. Solid black circles represent the data obtained from high- $P$  neutron-diffraction experiments ( $0$ – $2 \text{ GPa}$ ). (b) Isothermal volume-pressure data collected using energy-dispersive synchrotron XRD in a large-volume apparatus. The inset presents the isothermal bulk modulus as a function of temperature. All volume-pressure data fitted to the third-order Birch-Murnaghan equation of state with fixed  $B' = 4$ .<sup>26</sup>

The extended structural stability observed in this paper for stoichiometric *c*-CrN allows the bulk modulus to be determined more accurately based on the pressure-volume measurements, which are illustrated in Fig. 3. The  $B_0$  values, derived from the DAC data using a Birch-Murnaghan equation of state,<sup>26</sup> are  $253 (12) \text{ GPa}$  for *c*-CrN and  $262 (6) \text{ GPa}$  for *orthor*-CrN [Fig. 3(a)]. The relatively low  $B_0$  in *c*-CrN is further confirmed by our robust high- $P$ - $T$  synchrotron data, which lead to a more accurate value of  $B_0 = 257 (5) \text{ GPa}$  [Fig. 3(b)]. The temperature derivative of  $B_0$ ,  $(\partial B_0 / \partial T)_P$ , was determined for the *c*-CrN and was found to be  $-2.95 \times 10^{-2} \text{ GPa/K}$  [Inset in Fig. 3(b)]. In addition, the  $B_0$  derived from our experiments for *orthor*-CrN is in excellent agreement with the reported values in Refs. 10 and 11. These experimental findings support the computational model of Alling *et al.*,<sup>11</sup> indicating that atomic spin has a profound influence on the material’s elastic properties. Our results, however, do not reveal any phase-transition-induced elastic softening in CrN and, hence, invalidate the main conclusion and associated physical mechanisms reported by Rivadulla *et al.*<sup>10</sup> Conceivably, the controversies between experiments and nonmagnetic simulations for other paramagnetic materials CoO (Ref. 8) and  $\text{PbCrO}_3$  (Ref. 9) may also be resolved by computational models involving the local magnetic moment. Further computational efforts along this direction are required to establish the ubiquity of this phenomenon for the family of paramagnetic materials. We conclude that CrN may show complex structural, elastic, and magnetic behaviors depending on the sample preparation procedure and defect chemistry.

ACKNOWLEDGMENTS

This work has partly benefited from the use of the Lujan Neutron Scattering Center at Los Alamos Neutron Science Center, which is funded by the US Department of Energy’s Office of Basic Energy Sciences. This work was also supported

by the China 973 Program (Grant No. 2011CB808205) and the National Natural Science Foundation of China (Grant No. 11027405). We thank J. Zhou (The University of Texas, Austin) for the low-temperature electrical resistivity measurements. The use of HPCAT (at the 16BM-D beamline), APS is supported by the Carnegie Institute of Washington, Carnegie DOE Alliance Center, University of Nevada at Las Vegas, and Lawrence Livermore National Laboratory

through funding from the DOE-National Nuclear Security Administration, the DOE-Basic Energy Sciences, and the NSF; the APS is supported by the DOE-BES, under Contract No. DE-AC02-06CH11357. The use of the National Synchrotron Light Source (at the X17B2 beamline), Brookhaven National Laboratory, was supported by the US Department of Energy, Office of Science, Office of Basic Energy Sciences, under Contract No. DE-AC02-98CH10886.

---

\*Corresponding authors: duanweihe@scu.edu.cn, yusheng.zhao@unlv.edu

<sup>1</sup>L. M. Corliss, N. Elliott, and J. M. Hastings, *Phys. Rev.* **117**, 929 (1960).

<sup>2</sup>A. Filippetti and N. A. Hill, *Phys. Rev. Lett.* **85**, 5166 (2000).

<sup>3</sup>A. Filippetti, W. E. Pickett, and B. M. Klein, *Phys. Rev. B* **59**, 7043 (1999).

<sup>4</sup>A. Herwadkar and W. R. L. Lambrecht, *Phys. Rev. B* **79**, 035125 (2009).

<sup>5</sup>B. Alling, T. Marten, and I. A. Abrikosov, *Phys. Rev. B* **82**, 184430 (2010).

<sup>6</sup>J. Kunes, A. V. Lukoyanov, V. I. Anisimov, R. T. Scalettar, and W. E. Pickett, *Nature Mater.* **7**, 198 (2008).

<sup>7</sup>J. F. Lin, V. V. Struzhkin, S. D. Jacobsen, M. Y. Hu, P. Chow, J. Kung, H. Z. Liu, H. K. Mao, and R. J. Hemley, *Nature (London)* **436**, 377 (2005).

<sup>8</sup>J. F. Liu, Y. He, W. Chen, G. Q. Zhang, Y. W. Zeng, T. Kikegawa, and J. Z. Jiang, *J. Phys. Chem. C* **111**, 2 (2007).

<sup>9</sup>W. Xiao, D. Tan, X. Xiong, J. Liu, and J. Xu, *Proc. Natl. Acad. Sci. USA* **107**, 14026 (2010).

<sup>10</sup>F. Rivadulla *et al.*, *Nature Mater.* **8**, 947 (2009).

<sup>11</sup>B. Alling, T. Marten, and I. A. Abrikosov, *Nature Mater.* **9**, 283 (2010).

<sup>12</sup>V. M. Vinokur, T. I. Baturina, M. V. Fistul, A. Y. Mironov, M. R. Baklanov, and C. Strunk, *Nature (London)* **452**, 613 (2008).

<sup>13</sup>S.-H. Shim, A. Bengtson, D. Morgan, W. Sturhahn, K. Cataiii, J. Zhao, M. Lerche, and V. Prakapenka, *Proc. Natl. Acad. Sci. USA* **106**, 5508 (2009).

<sup>14</sup>J.-F. Lin *et al.*, *Nat. Geosci.* **1**, 688 (2008).

<sup>15</sup>T. Yamanaka, K. Hirose, W. L. Mao, Y. Meng, P. Ganesh, L. Shulenburg, G. Shen, and R. J. Hemley, *Proc. Natl. Acad. Sci. USA* **109**, 1035 (2012).

<sup>16</sup>F. Rivadulla *et al.*, *Nature Mater.* **9**, 284 (2010).

<sup>17</sup>M. Chen, S. M. Wang, J. Z. Zhang, D. W. He, and Y. S. Zhao, *Chem. Eur. J.*, doi:10.1002/chem.201202197.

<sup>18</sup>S. M. Wang *et al.*, *Chem. Mater* **24**, 3023 (2012); S. M. Wang, J. Z. Zhang, D. W. He, and Y. S. Zhao, *Inorg. Chem.* (to be published).

<sup>19</sup>B. H. Toby, *J. Appl. Crystallogr.* **34**, 210 (2001).

<sup>20</sup>P. A. Bhobe *et al.*, *Phys. Rev. Lett.* **104**, 236404 (2010).

<sup>21</sup>J. Z. Zhang and P. J. Kostak, *Phys. Earth Planet. Inter.* **129**, 301 (2002).

<sup>22</sup>Y. S. Zhao, R. B. von Dreele, and J. G. Morgan, *High Press. Res.* **16**, 161 (1999).

<sup>23</sup>D. L. Decker, *J. Appl. Phys.* **42**, 3239 (1971).

<sup>24</sup>J. D. Browne, P. R. Liddell, R. Street, and T. Mills, *Phys. Status Solidi A* **1**, 715 (1970).

<sup>25</sup>D. Gall, C. S. Shin, R. T. Haasch, I. Petrov, and J. E. Greene, *J. Appl. Phys.* **91**, 5882 (2002).

<sup>26</sup>F. Birch, *Phys. Rev.* **71**, 809 (1947).